Desalination and Water Treatment
www.deswater.com

doi: 10.1080/19443994.2015.1086898

57 (2016) 17646–17657
August

Taylor & Francis
Taylor & Francis Group

Preparation of ECTFE membranes with bicontinuous structure via TIPS method by a binary diluent

Bo Zhou, Qian Li, Yuanhui Tang, Yakai Lin, Xiaolin Wang*

Beijing Key Laboratory of Membrane Materials and Engineering, Department of Chemical Engineering, Tsinghua University, Beijing 10084, P.R. China, Tel. +86 010 62794741; Fax: +86 62794742; emails: zhoubo09@126.com (B. Zhou), qian-li@mail.tsinghua.edu.cn (Q. Li), tangyuanhui@126.com (Y. Tang), linyakai@tsinghua.org.cn (Y. Lin), xl-wang@tsinghua.edu.cn (X. Wang)

Received 18 March 2015; Accepted 20 August 2015

ABSTRACT

The ECTFE membrane with bicontinuous structure was prepared by a binary diluent via thermally induced phase separation method. The effect of binary diluent composition on membrane structure was investigated systematically. The Flory–Huggins interaction parameters between ECTFE and diluents were investigated to analyze the mechanism of phase separation. Dibutyl sebacate (DBS) was selected as the primary diluent due to the high boiling point and strong interaction with ECTFE, while triphenyl phosphite (TPP) was selected as the secondary diluent because of the good compatibility with DBS. As the weight ratio of DBS to TPP was 3/2, a uniform bicontinuous structure was obtained. A typical upper critical solution temperature behavior was displayed and the monotectic concentration was as high as approximately 50 wt.%. Finally, an ECTFE hollow fiber membrane with a bicontinuous structure was prepared by the binary diluent and revealed high mechanical strength (tensile strength of 2.40 MPa) and filtration performance (water flux of 313 L m^{-2} h^{-1} at 0.1 MPa).

Keywords: ECTFE; Bicontinuous structure; Thermally induced phase separation; Binary diluent; Hollow fiber

1. Introduction

Water scarcity is one of the most serious global challenges. Presently, over one-third of the world's population lives in water-stressed countries and this figure will predictably rise to nearly two-thirds by 2025 [1–3]. In the coming decades, surging population growth, urban development, and industrialization will increase worldwide demand for fresh water. The available method to increase water supply is to capture water directly from non-traditional sources such as industrial or municipal wastewaters. Membrane processes are promising technologies for wastewater treatment because of their advantages such as low-energy consumption and small amounts of additive needed [4,5].

Ethylene chlorotrifluoroethylene copolymer (ECTFE) has been recognized as one of the most promising materials in membrane industry because of its resistance to aggressive chemicals and excellent mechanical property [6,7]. Compared with polyvinylidene fluoride (PVDF) membranes which are most widely used in

*Corresponding author.

microfiltration and ultrafiltration processes, ECTFE membranes can bear much stronger and longer cleaning, indicating the longer membrane lifetime. Due to its high stability, ECTFE membranes are hardly prepared via the nonsolvent-induced phase separation method [8]. Thermally induced phase separation (TIPS) method is another promising technique for the preparation of polymeric porous membranes by controlling phase separation [9–12]. It has been reported that ECTFE membranes were prepared by TIPS method above a temperature of 220˚C [13–15].

Bicontinuous structure is regarded as ideal membrane structure since it contributes to high porosity, water flux, and tensile strength [16,17]. ECTFE membranes with bicontinuous structure have been prepared by adding silica powder into the ECTFE–diluent system during TIPS process [18,19]. The hot NaOH solution was used to remove silica powder, which involves a complicated extraction process during the membrane preparation. Recently, ECTFE membranes with bicontinuous structure were prepared from the ECTFE–diethyl phthalate (DEP) system without the addition of inorganic particles [20]. The phase diagram of ECTFE–DEP system displays a typical upper critical solution temperature (UCST) behavior and the monotectic concentration is approximately 55 wt.%. Bicontinuous structure of the ECTFE membranes is obtained at the ECTFE concentration from 10 to 50 wt.%. However, the boiling point of DEP (295˚C) is slightly higher than the temperature of membrane preparation (250˚C). As a result, evaporation of DEP occurs severely during the TIPS process. In short, it is difficult to prepare ECTFE membranes with high performance via TIPS method by a unary diluent.

In our preceding works, the binary diluent comprised of a primary diluent and a secondary diluent has been used to create liquid–liquid (L–L) phase separation. The resultant PVDF and polypropylene (PP) membranes with bicontinuous structure are obtained [21–23]. The effect of the binary diluent on PP membrane formation has been investigated by dissipative particle dynamics simulation. The primary diluent should have good compatibility with the polymer, while the secondary diluent should have good compatibility with the primary diluent but poor compatibility with the polymer. Consequently, with the addition of the secondary diluent, the cloud-point temperature of the PP-binary diluent system is shifted to a higher temperature, resulting in the membrane structure changing from spherulitic to bicontinuous.

In this work, ECTFE membranes with bicontinuous structure are prepared from the ECTFE–binary diluent system via TIPS method. Firstly, the effect of diluent composition on membrane structure is investigated to select the suitable primary and secondary diluents. The Flory–Huggins interaction parameters between ECTFE and diluents are investigated to analyze the mechanism of phase separation. Then, the weight ratio of the primary diluent to the secondary diluent is optimized to obtain the ECTFE membranes with uniform bicontinuous structure. Finally, the ECTFE hollow fiber membrane with bicontinuous structure will be prepared by a binary diluent and the performance of the ECTFE hollow fiber membrane will be measured and discussed.

2. Experimental

2.1. Materials

Ethylene chlorotrifluoroethylene copolymer, Halar® ECTFE (Grade 902), was purchased from Solvay. Benzyl benzoate (BB), diethyl phthalate (DEP), dibutyl phthalate (DBP), dibutyl sebacate (DBS), hexadecanol (HDC), triphenyl phosphite (TPP), oleic acid (OA), tetraethylene glycol (TEG), and bovine serum albumin (BSA, M_w = 66,000) were purchased from Sinopharm Chemical Reagent Co., Ltd. The BSA was stored at 2–8˚C before use.

2.2. Determination of phase diagram

The cloud-point temperature of the ECTFE–diluent system was defined as the temperature below which the solution became turbid. It was obtained by an optical microscopy (Olympus BX51). The blend sample of ECTFE and the diluent prepared via previously described method [24,25] was sandwiched between a pair of glass microscope cover slips which were sealed with silicone rubber to prevent the evaporation of the diluent. Then, the sample was placed on a hot stage (Linkam THMS 600) at 250˚C for 5 min and cooled to 40˚C at a controlled rate of 10˚C/min.

The crystallization temperature was determined by differential scanning calorimetry (DSC, TA Q200). The blend sample of ECTFE and the diluent was melted at 250˚C for 5 min, and then cooled at 10˚C/min to 40˚C. The peak of the DSC curve was regarded as the crystallization temperature.

2.3. Preparation of ECTFE membranes

2.3.1. ECTFE membrane samples

Unary diluents and binary diluents were used to prepare ECTFE membrane samples via TIPS method, respectively. ECTFE and the diluent were melt-blended in a vessel at an elevated temperature (250˚C)

to obtain a homogeneous solution. Phase separation was induced by quenching the solution in ice water. The diluent in the blend sample was extracted by ethanol and the ECTFE membrane samples were obtained after the volatilization of ethanol [16,24–26].

2.3.2. ECTFE hollow fiber membranes

The ECTFE hollow fiber membranes were prepared from the ECTFE–binary diluent system via TIPS method. The binary diluent consisted of DBS and TPP. ECTFE (20 wt.%), DBS (48 wt.%), and TPP (32 wt.%) were melt-blended in a twin screw extruder at an elevated temperature (210–250°C) to obtain a homogeneous solution. The hollow fiber was extruded from the spinneret at the end of the extruder and then immersed into a water bath at 50°C to induce phase separation. After that, the solidified hollow fiber membrane was wound on a take-up roller. Glycerol was employed as bore liquid at 200°C. The air gap was kept at 2 mm above the water bath. The diluent was extracted by ethanol and the ECTFE hollow fiber membrane was obtained after the volatilization of ethanol.

2.4. Characterization of ECTFE membranes

2.4.1. Morphologies

The morphologies of ECTFE membranes were examined using a scanning electron microscope (SEM, JEOL JSM7401). ECTFE membranes were fractured in liquid nitrogen and coated with platinum. The SEM with the accelerating voltage set to 1.0 or 3.0 kV was used to examine the cross-section and surface morphologies of membranes.

2.4.2. Porosity and mean pore size

Porosity (ε, %) of ECTFE hollow fiber membranes was determined by gravimetric measurements of the difference between dry and fully isobutanol-filled membranes [27]:

$$\varepsilon = (m_1 - m_2)/\rho_i/((m_1 - m_2)/\rho_i + m_2/\rho_p) \quad (1)$$

where m_1 is the weight of the wet membrane (g); m_2 is the weight of the dry membrane (g), ρ_i is the isobutanol density (0.806 g cm^{-3}); and ρ_p is the polymer density (1.71 g cm^{-3}).

The mean pore radius r_m of the hollow fiber membrane was determined by the filtration velocity method. According to Guerout–Elford–Ferry equation, r_m (nm) could be calculated [28] as:

$$r_m = ((2.9 - 1.75\varepsilon)8000\eta lq/(\varepsilon A\Delta P))^{1/2} \quad (2)$$

where η is the water viscosity (8.9×10^{-4} Pa s); l is the membrane thickness (m); q is the volume of the permeation water per unit time (m^3 s^{-1}); A is the effective area of the membrane (m^2); and ΔP is the operation pressure (0.1 MPa).

2.4.3. Membrane strength

The tensile strength of the hollow fiber membrane was measured by a universal testing machine (Shimadzu AGS-100A) equipped with a 5-kg load cell. Each sample was stretched at a constant rate of 25 mm/min. The initial distance between the clamps was 50 mm. Five specimens were tested for each sample.

2.4.4. Filtration performance

The pure water flux and rejection to BSA of the ECTFE hollow fiber membrane were determined by a self-made dead-end filtration under the pressure of 0.1 MPa. The flux (J_v, L m^{-2} h^{-1}) was calculated by the following equation [29]:

$$J_v = m/(\rho A\Delta t) \quad (3)$$

where m, ρ, A, and Δt are the permeation mass (g), water density (g m^{-3}), outside surface area of the membrane (m^2), and permeation time (h), respectively.

The same setup above was used for rejection experiments with BSA at the concentration of 0.5 g/L. The concentrations of BSA in the feed and permeation solutions were measured by an ultraviolet–visible spectrophotometer (TU-1810, China) at 280 nm. The rejection (R, %) was calculated by the following equation:

$$R = (1 - C_P/C_F) \times 100 \quad (4)$$

where C_P and C_F are the protein concentrations in the permeation and feed solutions, respectively.

3. Results and discussion

3.1. Formation of ECTFE membranes with bicontinuous structure

3.1.1. ECTFE–unary diluent system

In order to obtain a suitable binary diluent to create L–L phase separation, the primary diluent should

be the one having good compatibility with the polymer [22,23]. Several common chemicals with the solubility parameter from 18.8 to 21.3 $MPa^{1/2}$ were used as unary diluents to determine the suitable primary diluent. Thermodynamic phase diagram for the ECTFE–diluent systems with different unary diluents is shown in Fig. 1. The overall feature in Fig. 1 can be analyzed in terms of the interaction between ECTFE and the unary diluent. The Flory–Huggins interaction parameter (χ), typically used to interpret the interaction between ECTFE and the unary diluent, is calculated from the differences of the solubility parameter between ECTFE and the unary diluent as listed in Table 1. The Flory–Huggins interaction parameter (χ) between ECTFE and DBS is lowest, indicating good compatibility of the system. Thus, only solid–liquid (S–L) phase separation occurs (Fig. 1(a)), resulting in the spherulitic structure (Fig. 2(a)). With an increase in the Flory–Huggins interaction parameter (χ) between ECTFE and the unary diluent, compatibility of the ECTFE–diluent system becomes poorer. Consequently, the mechanism of phase separation changes from S–L to L–L [30–32] indicating that the resultant structure of ECTFE membranes changes from spherulitic to bicontinuous (Fig. 2). When DBP is used as the diluent, the membrane exhibits a structure mixed of spherulitic structure and bicontinuous structure (Fig. 2(b)). This is attributed to the narrow gap between the cloud-point temperature and the crystallization temperature [14,33]. In the cooling process, the L–L phase separation occurs simultaneously with polymer crystallization. When DEP is used as the diluent, the gap between the cloud-point temperature and the crystallization temperature is large (Fig. 1(c)), resulting in the uniform bicontinuous structure (Fig. 2(c)). The membrane prepared from the ECFTE–BB system shows irregular structure (Fig. 2(d)) due to the much poorer compatibility of the system. Meanwhile, the boiling point of DBS is the highest among the four diluents, indicating less evaporation of the diluent. Therefore, DBS is selected as the primary diluent because of the high boiling point and the low Flory–Huggins interaction parameter with ECTFE.

3.1.2. ECTFE–binary diluent system

In order to obtain ECTFE membranes with bicontinuous structure, a suitable secondary diluent should be added into the ECTFE–DBS system to alter the phase separation. Four nonsolvents of ECTFE including HDC, TPP, OA, and TEG are used as the secondary diluents to weaken the interaction between ECTFE and diluents. The different secondary diluents lead to the difference in membrane structure as shown in Fig. 3. As HDC or TEG is used as the secondary diluent, the big holes (Fig. 3(a) and (d)) appear in the membrane structure. When OA or TPP is used as the secondary diluent, the resultant membrane shows a typical bicontinuous structure (Fig. 3(b) and (c)). As reported in our preceding work [37], the phase separation is significantly influenced by the interaction between the primary diluent and the secondary diluent. The secondary diluent is firstly separated from the homogenous solution of the polymer–binary diluent system when the interaction between the primary diluent and the secondary diluent is weak, resulting in an irregular structure (Fig. 3(a) and (d)). Thus, the secondary diluent should have good compatibility with the primary diluent but poor compatibility with ECTFE. According to the solubility parameters in Table 1, the solubility parameters (δ) of OA (19.3 $MPa^{1/2}$) and TPP (19.0 $MPa^{1/2}$) are much closer to that of DBS (18.8 $MPa^{1/2}$), indicating the superior compatibility of the binary diluents. Thus, a bicontinuous structure is obtained when OA or TPP is used as the secondary diluent. Nevertheless, OA containing

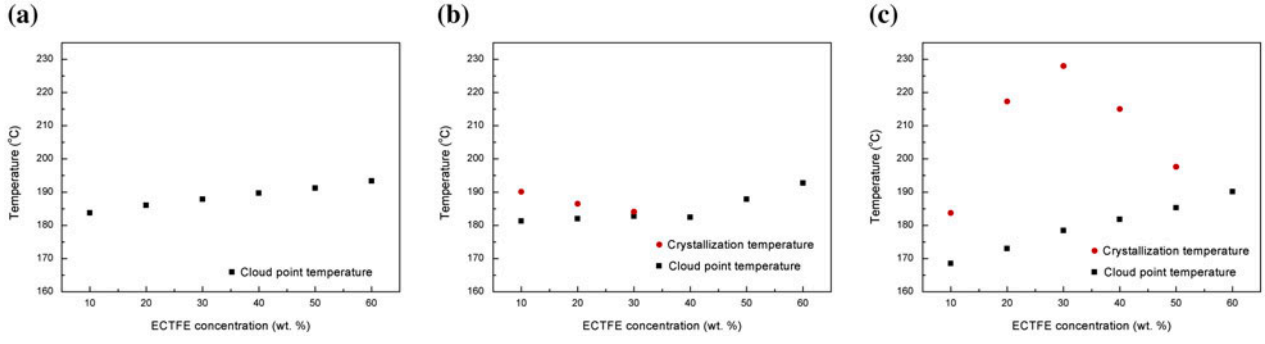

Fig. 1. Thermodynamic phase diagram for the ECTFE–diluent systems with different unary diluents: (a) DBS, (b) DBP, and (c) DEP.

Table 1
Properties of ECTFE and diluents

Polymer and diluents	V^a (cm^3/mol)	$T_m{}^b$ (℃)	$T_b{}^b$ (℃)	$T_f{}^b$ (℃)	δ^d ($MPa^{1/2}$)	χ^f
ECTFE	–	220–230[c]	–	–	17.3[e]	–
BB	188	21	323	148	21.3	1.55
DEP	199	−3	295	140	20.5	1.16
DBP	266	−35	340	171	19.0	0.66
DBS	337	1	344	177	18.8	0.64
HDC	299	49	334	135	17.8[e]	–
TPP	262	22	360	218	19.0	–
OA	316	13	360	189	19.3[e]	–
TEG	173	−6	307	176	20.3	–

Notes: V, molar volume; T_m, melting point; T_b, boiling point; T_f, flash point; χ, Flory–Huggins interaction parameter between ECTFE and diluent at 298 K; δ, solubility parameter at 298 K.

[a]Calculated by Advanced Chemistry Development (ACD/Labs) Software V11.02 (©1994–2015 ACD/Labs).

[b]Data from the Ref. [34].

[c]Data from Solvay.

[d]Data from the Ref. [35].

[e]Calculated by molecular dynamics simulation [20,36].

[f]χ can be related to δ: $\chi = 0.34 + V_i(\delta_i - \delta_j)^2/RT$, where i and j respectively denotes diluent and polymer.

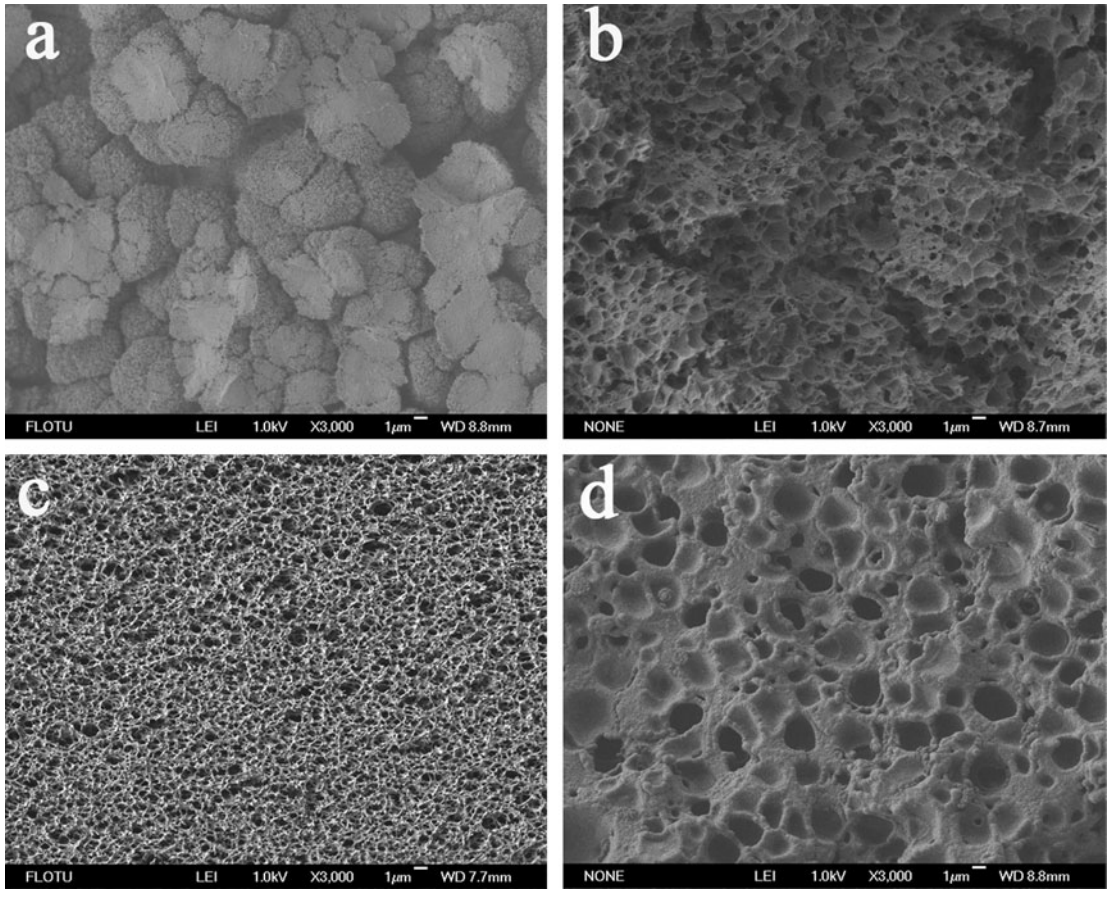

Fig. 2. Cross section morphologies of ECTFE membranes prepared by various unary diluents at the ECTFE concentration of 30 wt.%: (a) DBS, (b) DBP, (c) DEP, and (d) BB.

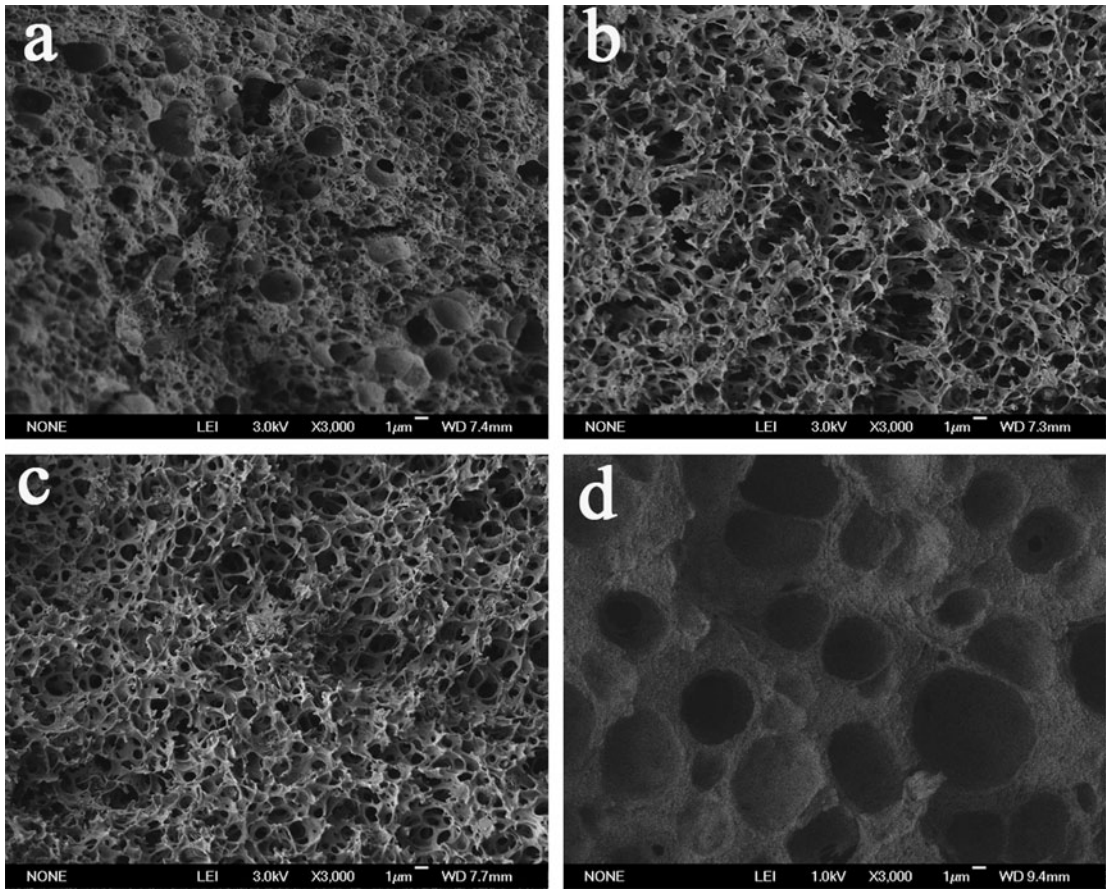

Fig. 3. Cross section morphologies of ECTFE membranes prepared by various secondary diluents: (a) HDC, (b) TPP, (c) OA, and (d) TEG. (ECTFE concentration: 30 wt.%; primary diluent: DBS; weight ratio of DBS to the secondary diluent: 3/2.)

unsaturated double bonds is extremely easy to oxidize at an elevated temperature. As a result, TPP is chosen as the secondary diluent in the following study.

As shown in Fig. 4, the phase diagram of the ECTFE–binary diluent system displays an UCST behavior as the weight ratio of DBS to TPP is 3/2. The L–L phase separation region is large and the monotectic concentration is approximately 50 wt.%. Additionally, the crystallization temperature of the ECTFE–binary diluent system (Fig. 4) is higher than that of the ECTFE–DBS system (Fig. 1(a)). The higher crystallization temperature of the polymer–diluent system indicates a lower degree of super cooling or a lower driving force needed for polymer crystallization. As reported, the weak interaction between polymer and diluent leads to the high mobility of polymer segments and enhances crystal nucleation and growth of polymer [26,38]. As a result, the ECTFE–binary system with lower interaction needs lower degree of the super cooling to form the crystal nuclei of ECTFE and the crystallization temperature increases with the addition of TPP.

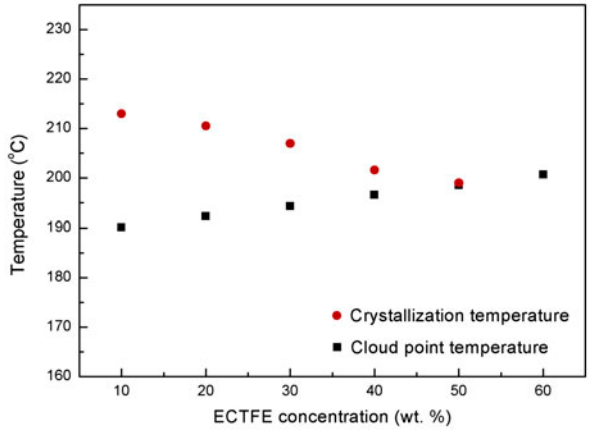

Fig. 4. Thermodynamic phase diagram for the ECTFE–binary diluent system. (Weight ratio of DBS to TPP: 3/2.)

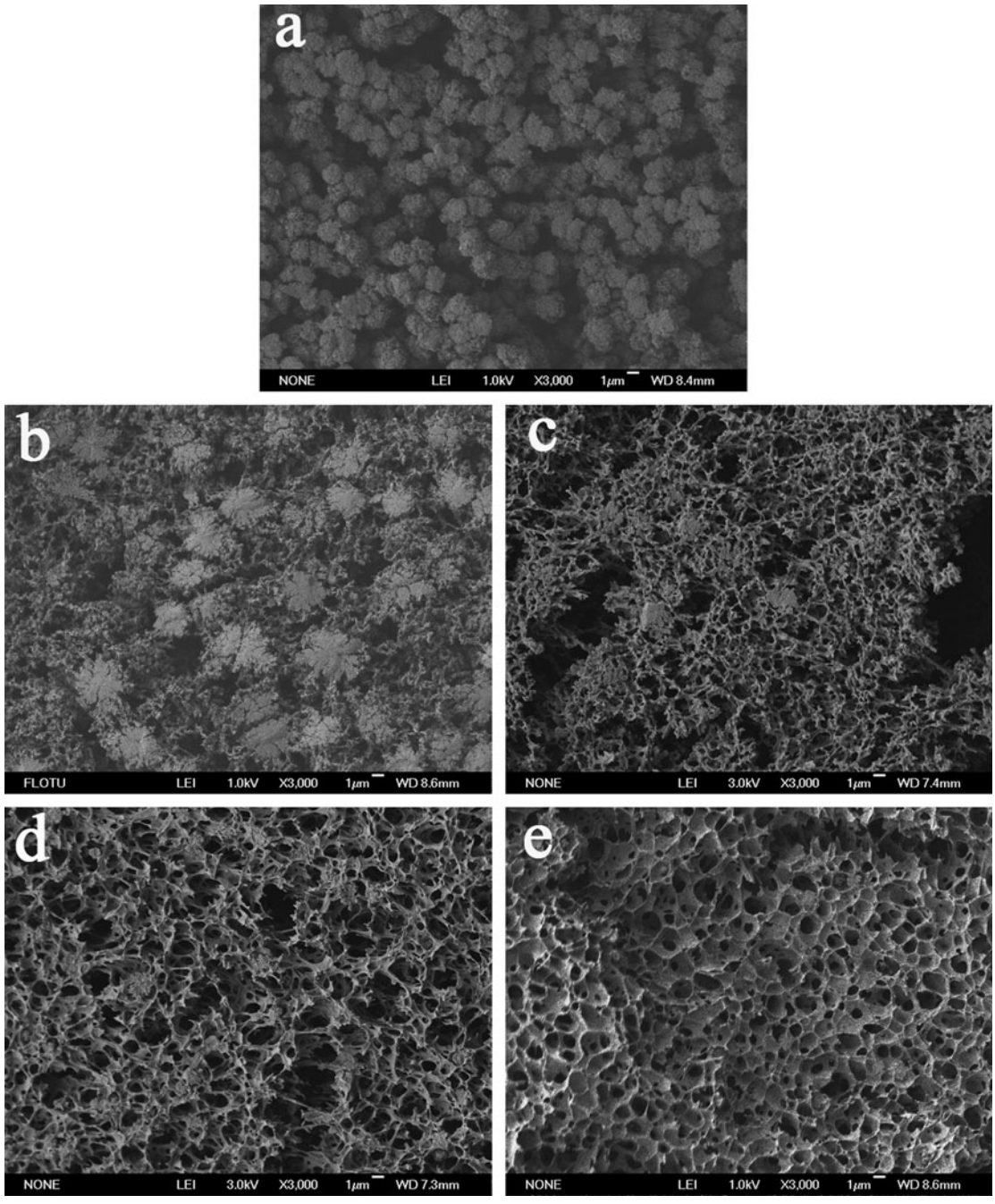

Fig. 5. Cross section morphologies of ECTFE membranes prepared by binary diluents with various weight ratios of DBS to TPP: (a) 1/0, (b) 4/1, (c) 7/3, (d) 3/2, and (e) 1/1. (ECTFE concentration: 30 wt.%.)

The evolution in membrane structure via TIPS method is closely related to thermodynamics of the phase separation process [39]. As mentioned above, the mechanism of phase separation is greatly influenced by the interaction between ECTFE and diluents. The membrane structure is also affected by the weight ratio of DBS to TPP. Typical spherulitic structure (Fig. 5(a)) is obtained due to the S–L phase separation when the weight ratio of DBS to TPP is 1/0. With a decrease in the weight ratio of DBS to TPP, the spherulitic structure disappears and is replaced by the bicontinuous structure gradually. This is attributed to the mechanism of phase separation changing from S–L to L–L as well as the expanding L–L phase separation

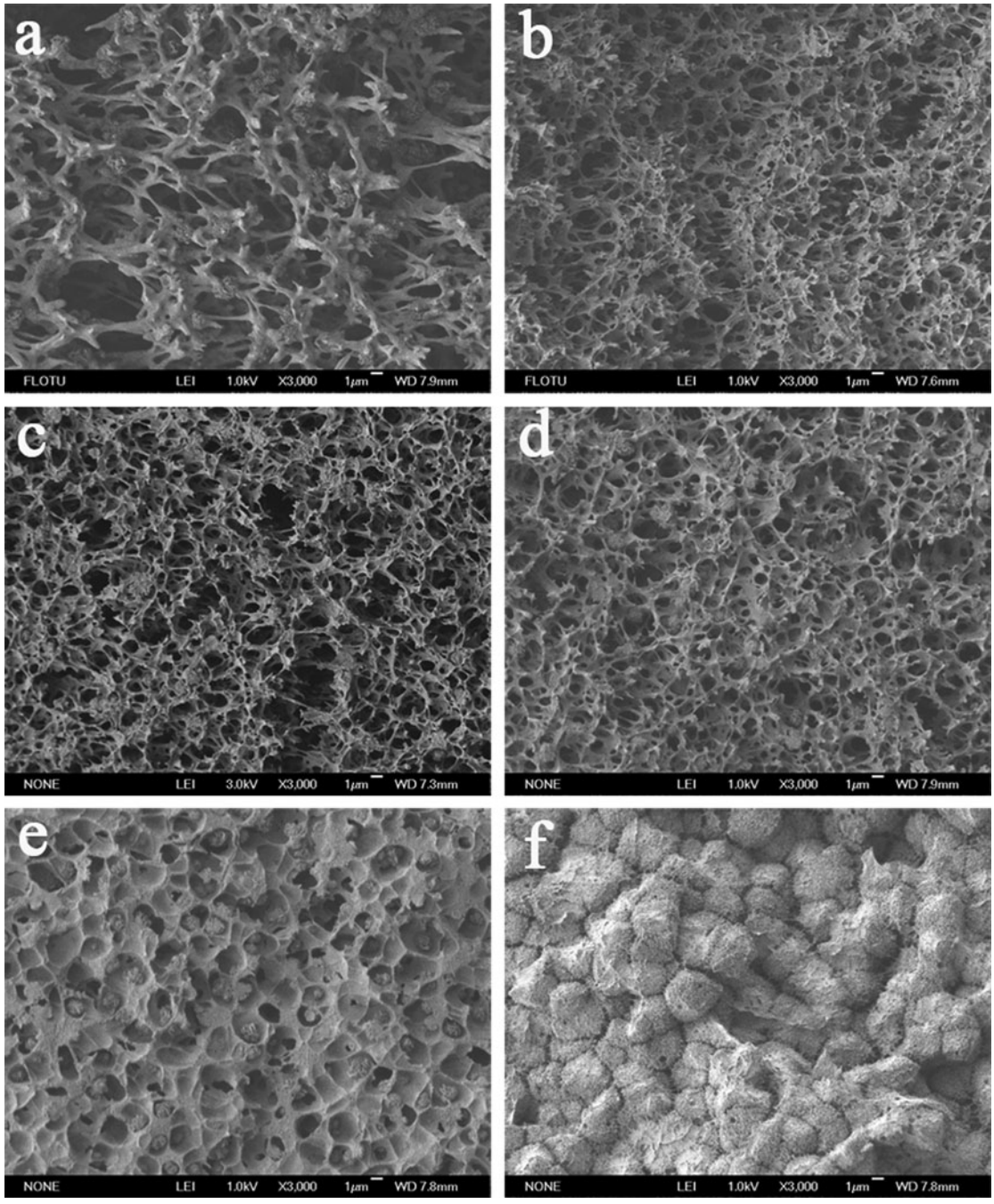

Fig. 6. Cross section morphologies of ECTFE membranes prepared from ECTFE–binary diluent systems with various ECTFE concentrations: (a) 10 wt.%, (b) 20 wt.%, (c) 30 wt.%, (d) 40 wt.%, (e) 50 wt.%, and (f) 60 wt.%. (Weight ratio of DBS to TPP: 3/2.)

region. Nevertheless, when the weight ratio of DBS to TPP is 1/1, the membrane with cellular structure is obtained due to the much poorer compatibility of the ECTFE–binary diluent system. Thus, 3/2 is the optimum weight ratio to prepare the ECTFE membrane with bicontinuous structure. Consequently, the weight ratio of DBS to TPP is 3/2 in the following study.

The phase separation is also significantly influenced by the polymer concentration, resulting in different membrane structure and performance. Fig. 6 shows the cross section morphologies of ECTFE membranes prepared with various ECTFE concentrations. When the ECTFE concentration is above the monotectic concentration (approximately 50 wt.%), only S–L

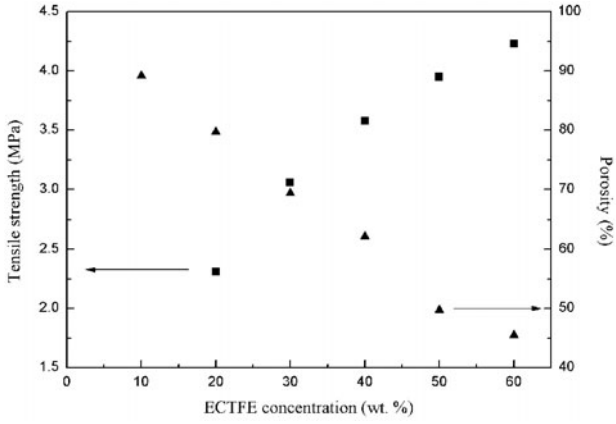

Fig. 7. Tensile strength and porosity of ECTFE membranes prepared from ECTFE–binary diluent systems with various ECTFE concentrations. (Weight ratio of DBS to TPP: 3/2.)

phase separation occurs, resulting in typical spherulitic structure (Fig. 6(f)). When the ECTFE concentration ranges from 10 to 50 wt.%, L–L phase separation with subsequent polymer crystallization occurs. The system enters an unstable or a metastable region. The phase separation proceeds through nucleation and growth in the metastable region, whereas it occurs through spinodal decomposition in the unstable region [39]. The system is divided into two phases, rich-polymer phase and lean-polymer phase. The rich-polymer phase solidifies as well as the structure is formed when the temperature of the system is below that of crystallization. As the ECTFE concentration is 10 or 50 wt.%, the homogeneous solution resides within the meta-stable region and phase separation occurs by nucleation and growth. The homogeneous solution with the ECTFE concentration of 10 wt.% consists of a small volume fraction of the rich-polymer phase dispersed in a lean-polymer phase, leading to the clear beads string structure (Fig. 6(a)). The opposite applies for the homogeneous solution with the ECTFE concentration of 50 wt.% resulting in the typical cellular structure (Fig. 6(e)). When the ECTFE concentration ranges from 20 to 40 wt.%, the phase separation process is determined by spinodal decomposition. Phase separation proceeds instantaneously and results in the regular bicontinuous structure (Fig. 6(b)–(d)). The tensile strength and porosity of ECTFE membranes prepared with various ECTFE concentrations are shown in Fig. 7. When the ECTFE concentration is 10 wt.%, the resultant membrane is brittle due to the clear beads string structure. With the ECTFE concentration increasing from 20 to 60 wt.%, the tensile strength

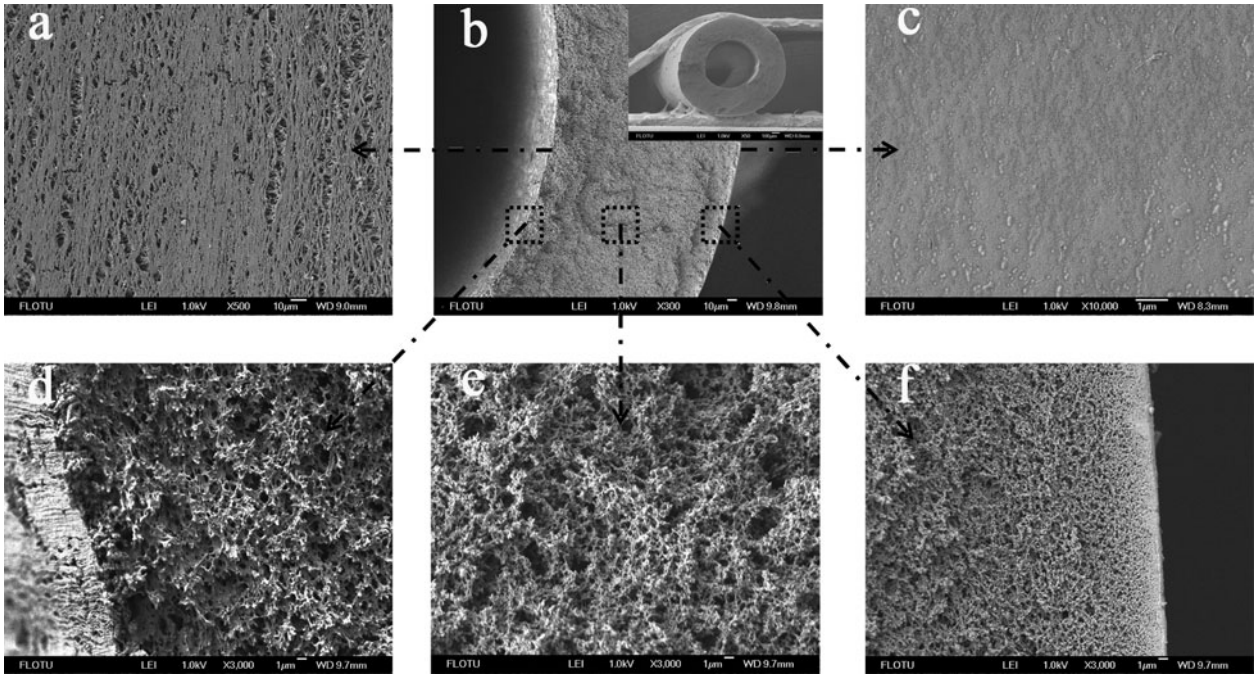

Fig. 8. Morphologies of the ECTFE hollow fiber membrane prepared at the ECTFE concentration of 20 wt.%. (a) Inner surface 500×, (b) cross section 300×, (c) outer surface 10,000×, (d) cross section near inner surface 3,000×, (e) inner surface 3,000×, and (f) cross section near outer surface 3,000×.

Table 2
Performance of the ECTFE hollow fiber membrane prepared at the ECTFE concentration of 20 wt.%

ID/OD (mm)	J_v (L m^{-2} h^{-1}, 0.1 MPa)	R (%)	ε (%)	r_m (nm)	Tensile strength (MPa)
1.03/0.65	313 ± 35	67.8 ± 5.3	81.2 ± 3.2	46.3 ± 2.5	2.40 ± 0.16

increases from 2.3 to 4.2 MPa. Nevertheless, the porosity of ECTFE membranes decreases from 89 to 45% when the ECTFE concentration increases from 10 to 60 wt.%.

3.2. Performance of the ECTFE hollow fiber membrane

In this work, it is the first time to prepare an ECTFE hollow fiber membrane with bicontinuous structure by a binary diluent. Fig. 8 shows the morphologies of ECTFE hollow fiber membranes prepared from the ECTFE–binary diluent system at the ECTFE concentration of 20 wt.%. The cross section morphologies of the ECTFE hollow fiber membrane are shown in Fig. 8(b) and (e). As described in the former section, the bicontinuous structure of the ECTFE hollow fiber membrane is obtained since the homogeneous solution resides within the unstable region and phase separation occurs by spinodal decomposition. Fig. 8(c) and (f) shows the outer surface morphology and cross section morphology near the outer surface. A skin layer with small pores is formed near the outer surface. The formation of the skin layer depends on several factors including the evaporation of the diluent, the rapid cooling rate as well as the low surface energy of ECTFE, which result in enrichment of ECTFE near the outer surface. Fig. 8(a) and (d) shows the inner surface morphology and the cross section morphology near the inner surface. As the experiment described, Glycerol at 200℃ is employed as bore liquid while the outer surface is immersed in the water bath (50℃). Thus, the cooling rate near the inner surface is slower than that near the outer surface. Meanwhile, the bore liquid prevents the evaporation of the diluent. As a result, there is no skin layer near the inner surface and the pore size and porosity of the inner surface are much higher than those of the outer surface.

The performances of the ECTFE hollow fiber membrane are listed in Table 2. The porosity and tensile strength of the membrane are as high as 81.2% and 2.40 MPa, respectively. This is attributed to the ideal bicontinuous structure. The pure water flux and rejection to BSA of the ECTFE hollow fiber membrane is more than 300 L m^{-2} h^{-1} and 65% at the operation pressure of 0.1 MPa. In short, an ECTFE hollow fiber membrane with the high performance is prepared via TIPS method by a binary diluent.

4. Conclusions

The ECTFE membranes with bicontinuous structure were prepared from ECTFE–binary diluent system via TIPS method. DBS with a high boiling point and good compatibility with ECTFE was chosen as the primary diluent. TPP with good compatibility with DBS but poor compatibility with ECTFE was used as the secondary diluent. As the weight ratio of DBS to TPP decreased, the interaction between ECTFE and the binary diluent became weaker, which was accompanied by an extension of L–L phase separation region. Uniform bicontinuous structure was obtained as the weight ratio of DBS to TPP was 3/2. The ECTFE hollow fiber membrane with bicontinuous structure was initially prepared by a binary diluent and showed high tensile strength of 2.40 MPa and water flux of 313 L m^{-2} h^{-1} at 0.1 MPa. The conclusions are also beneficial to the preparation of other polymer membranes with bicontinuous structure. Nevertheless, the final membrane structure also depends on the kinetics of the phase separation process. In the future work, the effects of preparation conditions such as air gap, water bath temperature, and bore liquid temperature will be investigated to further improve the performance of ECTFE hollow fiber membranes.

Acknowledgments

The authors would like to thank National Key Technologies R&D Program of China (No. 2015BAE06B00) and Tsinghua University Initiative Scientific Research Program (20121088039).

Abbreviations

SEM — scanning electron microscope
ECTFE — ethylene chlorotrifluoroethylene copolymer
BB — benzyl benzoate
DEP — diethyl phthalate
DBP — dibutyl phthalate

DBS — dibutyl sebacate
HDC — hexadecanol
TPP — triphenyl phosphite
OA — oleic acid
TEG — tetraethylene glycol
BSA — bovine serum albumin
ε — porosity
m_1 — mass of the wet membrane
m_2 — mass of the dry membrane
ρ — density
r_m — mean pore radius
η — water viscosity
l — membrane thickness
q — volume of the permeation water per unit time
A — effective area of the membrane
ΔP — operation pressure
J_v — pure water flux
m — permeation mass
Δt — permeation time
R — rejection
C — protein concentrations

References

[1] M. Elimelech, W.A. Phillip, The future of seawater desalination: Energy, Technology, and the Environment, Science 333 (2011) 712–717.
[2] I.K. Kalavrouziotis, P. Kokkinos, G. Oron, F. Fatone, D. Bolzonella, M. Vatyliotou, D. Fatta-Kassinos, P.H. Koukoulakis, S.P. Varnavas, Current status in wastewater treatment, reuse and research in some mediterranean countries, Desalin. Water Treat. 53 (2015) 2015–2030.
[3] P.M. Stathatou, F.K. Gad, E. Kampragou, H. Grigoropoulou, D. Assimacopoulos, Treated wastewater reuse potential: Mitigating water scarcity problems in the Aegean islands, Desalin. Water Treat. 53 (2015) 3272–3282.
[4] Z. Cui, N.T. Hassankiadeh, S.Y. Lee, J.M. Lee, K.T. Woo, A. Sanguineti, V. Arcella, Y.M. Lee, E. Drioli, Poly(vinylidene fluoride) membrane preparation with an environmental diluent via thermally induced phase separation, J. Membr. Sci. 444 (2013) 223–236.
[5] G.M. Mazziotti di Celso, M. Prisciandaro, Wastewater reuse by means of UF membrane process: A comparison with Italian provisions, Desalin. Water Treat. 51 (2013) 1615–1622.
[6] J. Scheirs, Modern Fluoropolymers: High Performance Polymers for Diverse Applications, Wiley, New York, NY, 1997.
[7] A.M.M. Baker, J. Mead, Thermoplastics, in: C.A. Harper (Ed.), Modern Plastics Handbook, McGraw-Hill, New York, NY, 2000, pp. 1–92 (Chapter 1).
[8] H.J. Müller, A new solvent resistant membrane based on ECTFE, Desalination 199 (2006) 191–192.
[9] A.J. Castro, Method for Making Microporous Products, U.S. Patent 4,247,498, 1981, pp. 1–64.
[10] H. Matsuyama, M.M. Kim, D.R. Lloyd, Effect of extraction and drying on the structure of microporous polyethylene membranes prepared via thermally induced phase separation, J. Membr. Sci. 204 (2002) 413–419.
[11] K. Nakatsuka, Y. Ohmukai, T. Maruyama, H. Matsuyama, Analysis of solidification rate of polymer solutions during PVDF membrane fabrication via TIPS method, Desalin. Water Treat. 17 (2010) 275–280.
[12] T. Tanaka, T. Aoki, T. Kouya, M. Taniguchi, W. Ogawa, Y. Tanabe, D.R. Lloyd, Mechanical properties of microporous foams of biodegradable plastic, Desalin. Water Treat. 17 (2010) 37–44.
[13] E. Drioli, S. Santoro, S. Simone, G. Barbieri, A. Brunetti, F. Macedonio, A. Figoli, ECTFE membrane preparation for recovery of humidified gas streams using membrane condenser, React. Funct. Polym. 79 (2014) 1–7.
[14] I.J. Roh, S. Ramaswamy, W.B. Krantz, A.R. Greenberg, Poly(ethylene chlorotrifluoroethylene) membrane formation via thermally induced phase separation (TIPS), J. Membr. Sci. 362 (2010) 211–220.
[15] S. Ramaswamy, A.R. Greenberg, W.B. Krantz, Fabrication of poly (ECTFE) membranes via thermally induced phase separation, J. Membr. Sci. 210 (2002) 175–180.
[16] Y.K. Lin, Y.H. Tang, H.Y. Ma, J. Yang, Y. Tian, W.Z. Ma, X.L. Wang, Formation of a bicontinuous structure membrane of polyvinylidene fluoride in diphenyl carbonate diluent via thermally induced phase separation, J. Appl. Polym. Sci. 114 (2009) 1523–1528.
[17] W.Z. Ma, J. Zhang, B. Bruggen, X.L. Wang, Formation of an interconnected lamellar structure in PVDF membranes with nanoparticles addition via solid–liquid thermally induced phase separation, J. Appl. Polym. Sci. 127 (2013) 2715–2723.
[18] D. Mullette, H.J. Muller, Poly(ethylene chlorotrifluoroethylene) membranes, U.S. Patent 7,247,238, 2007, pp. 1–22.
[19] Y. Mutoh, M. Miura, Porous fluorine resin membrane and process for preparing the same, U.S. Patent 4,702,836, 1987, pp. 1–10.
[20] B. Zhou, Y.K. Lin, W.Z. Ma, Y.H. Tang, Y. Tian, X.L. Wang, Preparation of ethylene chlorotrifluoroethylene co-polymer membranes via thermally induced phase separation, Chem. J. Chin. Univ. 33 (2012) 2585–2590.
[21] Y.H. Tang, Y.K. Lin, W.Z. Ma, Y. Tian, J. Yang, X.L. Wang, Preparation of microporous PVDF membrane via tips method using binary diluent of DPK and PG, J. Appl. Polym. Sci. 118 (2010) 3518–3523.
[22] B. Luo, Z. Li, J. Zhang, X.L. Wang, Formation of anisotropic microporous isotactic polypropylene (iPP) membrane via thermally induced phase separation, Desalination 233 (2008) 19–31.
[23] Y. Su, C. Chen, Y. Li, J. Li, Preparation of PVDF membranes via TIPS method: The effect of mixed diluents on membrane structure and mechanical property, J. Macromol. Sci., Part A 44 (2007) 305–313.
[24] Y.K. Lin, G. Chen, J. Yang, X.L. Wang, Formation of isotactic polypropylene membranes with bicontinuous structure and good strength via thermally induced phase separation method, Desalination 236 (2009) 8–15.
[25] J. Yang, D.W. Li, Y.K. Lin, X.L. Wang, F. Tian, Z. Wang, Formation of a bicontinuous structure membrane of polyvinylidene fluoride in diphenyl ketone

diluent via thermally induced phase separation, J. Appl. Polym. Sci. 110 (2008) 341–347.
[26] W.Z. Ma, S. Chen, J. Zhang, X.L. Wang, W. Miao, Membrane formation of poly(vinylidene fluoride)/poly(methyl methacrylate)/diluents via thermally induced phase separation, J. Appl. Polym. Sci. 111 (2009) 1235–1245.
[27] H. Tao, J. Zhang, X. Wang, Effect of diluents on the crystallization behavior of poly(4-methyl-1-pentene) and membrane morphology via thermally induced phase separation, J. Appl. Polym. Sci. 108 (2008) 1348–1355.
[28] Q. Li, Z.L. Xu, L.Y. Yu, Effects of mixed solvents and PVDF types on performances of PVDF microporous membranes, J. Appl. Polym. Sci. 115 (2010) 2277–2287.
[29] Q. Li, B. Zhou, Q.Y. Bi, X.L. Wang, Surface modification of PVDF membranes with sulfobetaine polymers for a stably anti-protein-fouling performance, J. Appl. Polym. Sci. 125 (2012) 4015–4027.
[30] H. Matsuyama, M. Teramoto, S. Kudari, Y. Kitamura, Effect of diluents on membrane formation via thermally induced phase separation, J. Appl. Polym. Sci. 82 (2001) 169–177.
[31] D.R. Lloyd, S.S. Kim, K.E. Kinzer, Microporous membrane formation via thermally-induced phase separation. II. Liquid–liquid phase separation, J. Membr. Sci. 64 (1991) 1–11.
[32] M. Liu, Z.L. Xu, D.G. Chen, Y.M. Wei, Preparation and characterization of microporous PVDF membrane by thermally induced phase separation from a ternary polymer/solvent/non-solvent system, Desalin. Water Treat. 17 (2010) 183–192.
[33] Z.S. Yang, P.L. Li, L.X. Xie, Z. Wang, S.C. Wang, Preparation of iPP hollow-fiber microporous membranes via thermally induced phase separation with co-solvents of DBP and DOP, Desalination 192 (2006) 168–181.
[34] J.A. Dean, Lange's Handbook of Chemistry, McGraw-Hill, New York, NY, 1999.
[35] J.E. Mark, Physical Properties of Polymers Handbook, Springer, New York, NY, 2007.
[36] Z.L. Luo, J.W. Jiang, Molecular dynamics and dissipative particle dynamics simulations for the miscibility of poly(ethylene oxide)/poly(vinyl chloride) blends, Polymer 51 (2010) 291–299.
[37] Y.H. Tang, Y.D. He, X.L. Wang, Effect of adding a second diluent on the membrane formation of polymer/diluent system via thermally induced phase separation: Dissipative particle dynamics simulation and its experimental verification, J. Membr. Sci. 409–410 (2012) 164–172.
[38] G.L. Ji, B.K. Zhu, Z.Y. Cui, C.F. Zhang, Y.Y. Xu, PVDF porous matrix with controlled microstructure prepared by TIPS process as polymer electrolyte for lithium ion battery, Polymer 48 (2007) 6415–6425.
[39] I. Pinnau, B.D. Freeman, in: I. Pinnau, B.D. Freeman, Membrane Formation and Modification, American Chemical Society, Washington, DC, 1999, pp. 1–22.